Potent Inhibitors of the *Plasmodium falciparum* Enzymes Plasmepsin I and II Devoid of Cathepsin D Inhibitory Activity

Karolina Ersmark,[†] Isabella Feierberg,[‡] Sinisa Bjelic,[‡] Elizabeth Hamelink,[§] Fiona Hackett,[#] Michael J. Blackman,[#] Johan Hultén,[†] Bertil Samuelsson,[§] Johan Åqvist,[‡] and Anders Hallberg*[,†]

Department of Medicinal Chemistry, Uppsala University, BMC, Box 574, SE-751 23 Uppsala, Sweden, and Department of Cell and Molecular Biology, Uppsala University, BMC, Box 596, SE-751 24 Uppsala, Sweden, Division of Parasitology, National Institute for Medical Research, The Ridgeway, Mill Hill, London NW7 1AA, UK, and Medivir AB, Lunastigen 7, SE-141 44 Huddinge, Sweden

Received June 18, 2003

The hemoglobin-degrading aspartic proteases plasmepsin I (Plm I) and plasmepsin II (Plm II) of the malaria parasite *Plasmodium falciparum* have lately emerged as putative drug targets. A series of C_2-symmetric compounds encompassing the 1,2-dihydroxyethylene scaffold and a variety of elongated P1/P1′ side chains were synthesized via microwave-assisted palladium-catalyzed coupling reactions. Binding affinity calculations with the linear interaction energy method and molecular dynamics simulations reproduced the experimental binding data obtained in a Plm II assay with very good accuracy. Bioactive conformations of the elongated P1/P1′ chains were predicted and agreed essentially with a recent X-ray structure. The compounds exhibited picomolar to nanomolar inhibition constants for the plasmepsins and no measurable affinity to the human enzyme cathepsin D. Some of the compounds also demonstrated significant inhibition of parasite growth in cell culture. To the best of our knowledge, these plasmepsin inhibitors represent the most selective reported to date and constitute promising lead compounds for further optimization.

Introduction

It is estimated that nearly half of the population in the world lives in malaria-endemic areas. Of the four species of Plasmodium responsible for human malaria, *Plasmodium falciparum* is the most lethal. At a minimum, 500 million people are afflicted and between 1 and 3 million people die from the disease each year.[1] With no new effective therapy, it has been claimed that these numbers will be at least doubled in the next 20 years due to the rapid development of parasite drug resistance. Consequently, there is an urgent need for new therapies. Hemoglobin degradation appears to be essential for the survival of *P. falciparum*, and the enzymes involved in this process constitute new and promising targets for drug intervention.[2] At least four aspartic proteases have been identified to be active in the acidic food vacuole,[3] and among these plasmepsin I (Plm I) and plasmepsin II (Plm II) have been most extensively studied. These two enzymes, both engaged in the initial phase of the hemoglobin degradation, exhibit 73% sequence identity and appear structurally very similar in the active site region.[4,5] This suggests that contemporaneous inhibition by one single inhibitor may be feasible. However, since the human aspartic protease cathepsin D (Cat D) has a 35% sequence identity and even higher binding site homology with Plm II, selectivity problems are common.[6] A number of potent Plm II inhibitors have been identified encompassing different mimics of the tetrahedral intermediate in the enzymatic catalysis (e.g., compound **1**−**3**, Figure 1).[4,7−19] Some of these inhibitors were also reported to strongly inhibit Plm I.[7,11,15−18]

Recent molecular modeling studies, starting from a 3D structure of Plm II complexed with pepstatin A,[4] suggested to us that 1,2-dihydroxyethylene, which had successfully been used in HIV-1 protease inhibitors,[20,21] could provide an alternative tetrahedral intermediate mimicking scaffold in Plm II inhibitors.[17,19] Guided by binding affinity calculations, the optimal configuration at the four central carbon atoms of the core structure was predicted and experimentally confirmed to be *RRRR* (as in the reference compounds **4** and **5** in Table 1) and as deduced from one example, hydroxyindan seemed to constitute both a proper P2 and P2′ substituent in Plm II inhibitors (compound **6**).[19]

Previous investigations had suggested a continuous S1−S3 cleft[4] and a flexible Met75−Val82 flap region,[22] both with a potential capability to accommodate extended and/or large P1/P1′ residues. We herein report a study in which molecular dynamics simulations were used in combination with experimental data to assess the binding conformations and inhibition constants of a series derivatives comprising (a) the 1,2-dihydroxyethylene *RRRR* scaffold and (b) extended P1/P1′ arms as characteristic features (i.e., **8**−**22** in Table 1). Notably, the compounds also strongly inhibited Plm I and were essentially devoid of any Cat D inhibitory activity.

Results

Chemistry. The reference compounds **4**−**6** were prepared according to Ersmark et al.,[19] and compound **8** was prepared according to Alterman et al.[23] The

* Department of Medicinal Chemistry, Uppsala University, BMC, Box 574, SE-751 23 Uppsala, Sweden. E-mail: Anders.Hallberg@orgfarm.uu.se. Phone: +46−18 471 42 84, Fax: +46−18 471 44 74.
† Department of Medicinal Chemistry, Uppsala University.
‡ Department of Cell and Molecular Biology, Uppsala University.
# National Institute for Medical Research.
§ Medivir AB.

10.1021/jm030933g CCC: $27.50
Published on Web 12/09/2003

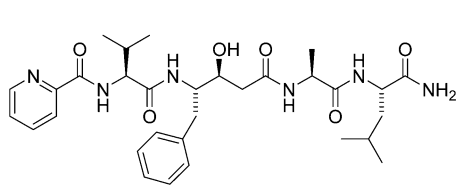

1. K_i Plm II, 0.56 nM; K_i Cat D, 21 nM
(Silva *et al.*[4])

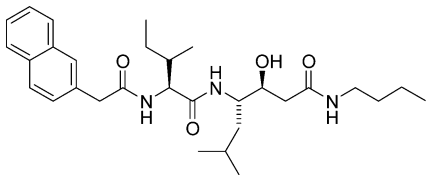

2. K_i Plm II, 50 nM; K_i Cat D, 320 nM
(Carroll *et al.*[8])

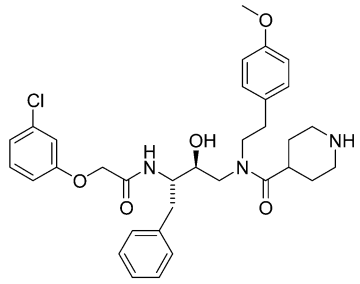

3. K_i Plm II, 4.3 nM; K_i Cat D, 63 nM
(Haque *et al.*[11])

Figure 1.

Scheme 1[a]

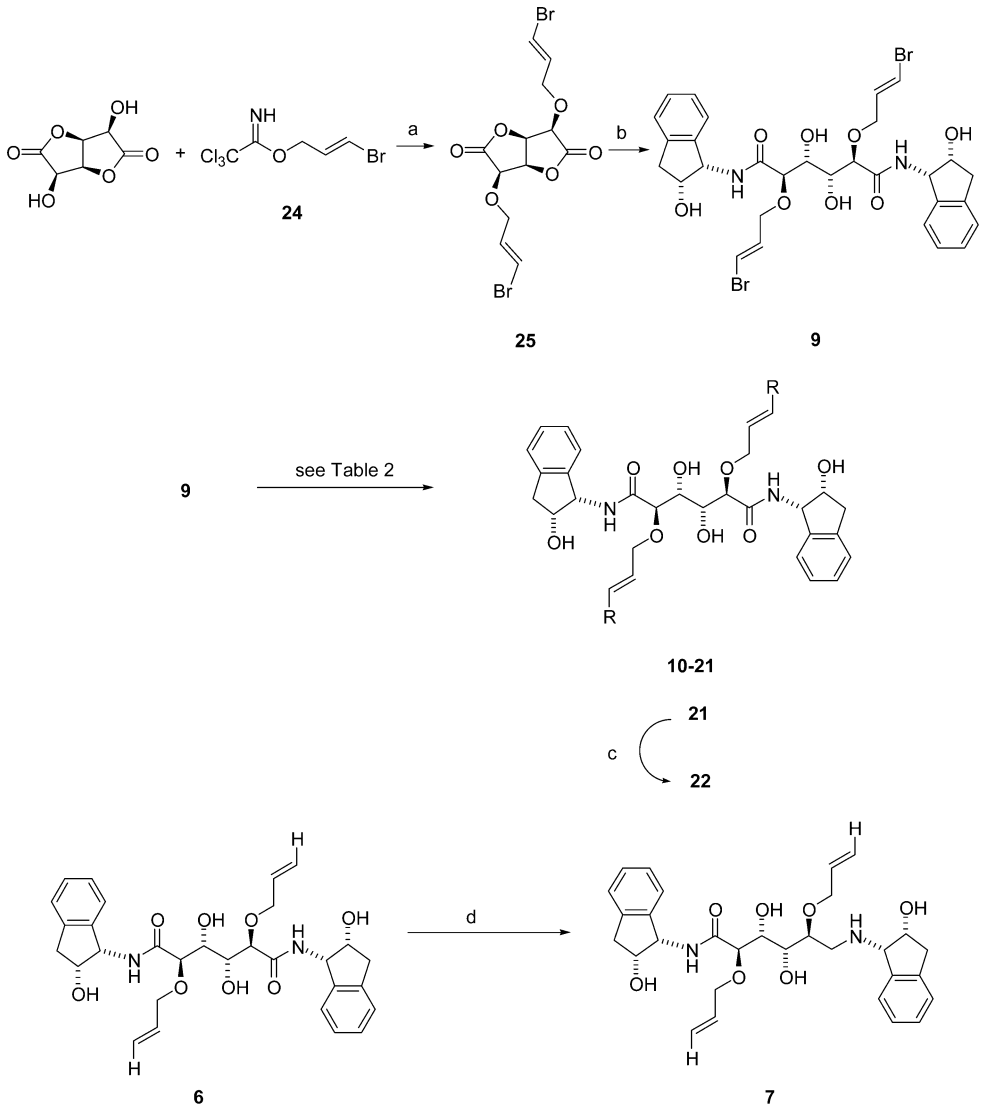

[a] (a) $BF_3 \times Et_2O$, dioxane; (b) (1*S*,2*R*)-1-amino-2-indanol, CH_2Cl_2, reflux; (c) $KF \times 2H_2O$, MeOH; (d) LAH, THF.

Table 1

Compound	Structure	Enzyme K_i (nM)				*P.falciparum* %inhi. @ 5 μM [a]
		Plm I [a]	Plm II		Cat D [a]	
			expt	calc [a]		
4	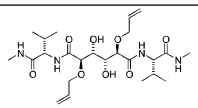	nd	4100 [b]	1100 [b]	nd	nd
5	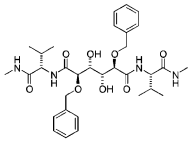	nd	3800 [b]	520 [b]	nd	nd
6	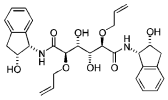	163	96 [b]	240 [b]	>2000	0
7	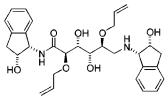	>1500	>2500	>2.4·10^7	>2000	50
8	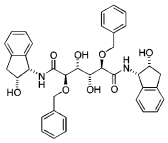	25	85	99	>2000	nd
9	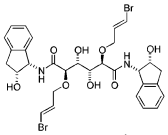	27	47	nd	>2000	nd
10	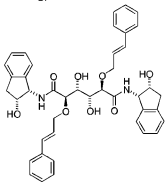	1.4	29	192	>2000	nd
11	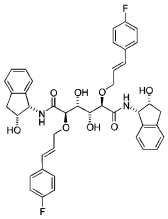	2.5	59	nd	>2000	nd
12	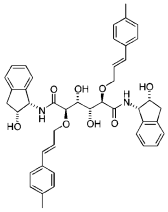	5.8	129	nd	>2000	nd
13	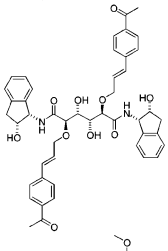	0.8	6	1.2	>2000	78
14	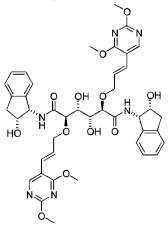	8.4	13	nd	>2000	2

Table 1 (Continued)

Compound	Structure	Enzyme K_i (nM)				*P.falciparum* %inhi. @ 5 μM [a]
		Plm I [a]	Plm II		Cat D [a]	
			expt	calc [a]		
15	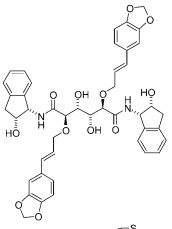	0.5	14	45	>2000	61
16	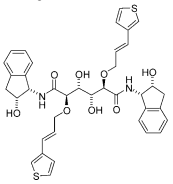	1.3	15	nd	>2000	nd
17	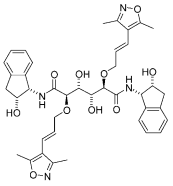	23	181	13	>2000	nd
18	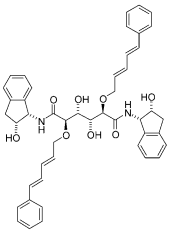	4.4	15	nd	>2000	nd
19	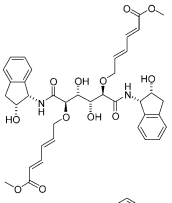	3.7	8.9	nd	>2000	51
20	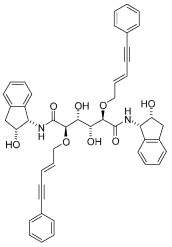	7.2	41	nd	>2000	nd
21	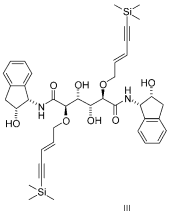	37	130	nd	>2000	nd
22	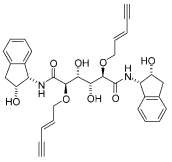	32	37	nd	>2000	nd
23	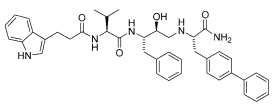	2.6 [c]	11 [c]	nd	30 [c]	56

[a] nd, not determined. [b] Data from ref 19. [c] Data from ref 18.

Table 2. Synthetic Methods for Preparation of the Analogues **10**−**21** with Extended P1/P1′ Arms

Compound	Reactant	Reaction medium	Time (min)	Temp. (°C)	R-group	Yield (%)
10	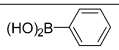	[a]	30	90		63
11	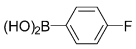	[a]	30	90	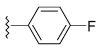	46
12	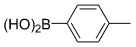	[a]	30	90	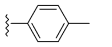	42
13	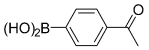	[a]	30	90	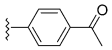	34
14	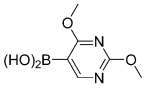	[a]	30	90	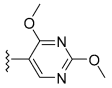	33
15	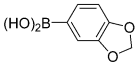	[a]	30	90	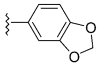	37
16	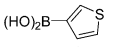	[a]	30	90	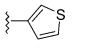	42
17	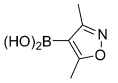	[a]	30	90	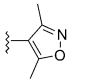	61
18		[b]	25	170	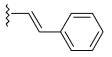	46
19		[b]	30	150	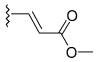	84
20		[c]	10	120	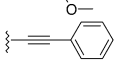	91
21		[c]	30	90		46

[a] $Pd(PPh_3)_4$, Na_2CO_3, DME, H_2O, EtOH. [b] Herrmann's catalyst,[26] $(i\text{-}Pr)_2EtN$, DMF, H_2O. [c] $Pd(PPh_3)_4$, Et_2NH, CuI, DMF.

diamide **9** was synthesized essentially following a previously reported strategy (Scheme 1).[23] Alkylation of the bislactone was accomplished using (*E*)-bromoallyl trichloroacetimidate **24** to give the (*E*)-bromobislactone **25** in 89% yield. Subsequent ring opening with (1*S*,2*R*)-1-amino-2-indanol afforded the (*E*)-bromodiamide **9** in 59% yield.

The analogues **10**−**21** with extended P1/P1′ arms (Scheme 1, Table 2) were prepared from the (*E*)-bromo precursor **9** by a series of different microwave-assisted palladium-catalyzed double coupling reactions.[24,25] A single-mode microwave cavity combined with a temperature and pressure feedback control system was employed, which made the procedure safe and reproducible. The Suzuki couplings to obtain **10**−**17** were conducted with a catalytic amount of tetrakis(triphenylphosphine)-palladium, 6 equiv of the appropriate organoboronic acid, and sodium carbonate as a base. Microwave irradiation at 90 °C for 30 min afforded the (*E*)-diamides **10**−**17** in 33−63% isolated yields. The two Heck vinylations delivering **18** and **19**, with styrene and methyl acrylate as olefinic substrates, respectively, were executed with the thermally stable Herrmann's catalyst[26] in aqueous DMF with diisopropylethylamine as a base. No regioisomers were observed. A time/temperature/pressure profile for the Heck vinylation of styrene to provide **18** is demonstrated in Figure 2. Initial attempts with tetrakis(triphenylphosphine)palladium or dichlorobis(triphenylphosphine)palladium as catalysts were unsuccessful in producing full conversion even at elevated temperatures (up to 150 °C). The Sonogashira reactions were performed using either phenylacetylene or trimethylsilylacetylene as coupling partners. These reactions were conducted in the presence of a catalytic amount tetrakis(triphenylphosphine)palladium and copper(I) in DMF. The enyne **20** was smoothly prepared in excellent yield (91%) by microwave irradiation at

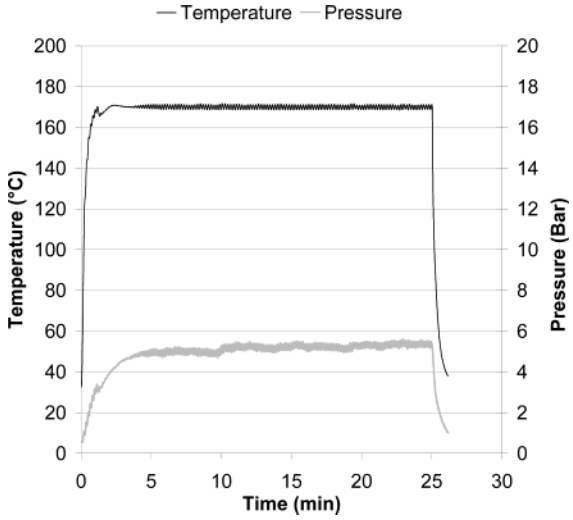

Figure 2. Time/temperature/pressure profile recorded from microwave heating of the Heck vinylation of styrene (Table 1, compound **18**).

120 °C for 10 min. Under the same reaction conditions, the less reactive trimethylsilylacetylene delivered partly the monocoupled product as deduced from analytical RP-LC-MS. By employing a longer reaction time in combination with a decrease in temperature (90 °C for 30 min) full conversion to the double coupled product **21** could be achieved. Deprotection of the trimethylsilyl group yielded (*E*)-diacetylene **22** (Scheme 1).

Reduction of **6**, formed via alkylation of the bislactone with allyl trichloroacetimidate,[19] to deliver **7** was accomplished with 4 equiv of lithium aluminum hydride (Scheme 1). The reaction mixture contained **7** as the main product, according to analytical RP-LC-MS. However, only a low yield (9%) of the product was isolated.

Enzyme Inhibition. To assess the activity and selectivity of the compounds, their inhibitory potencies

Table 3. Experimental and Calculated Energetics of Inhibition of Plm II

compound	$\Delta G_{bind,\,exp}$ (kcal/mol)[a]	$\Delta G_{bind,\,calc}$ (kcal/mol)	ligand-surrounding interactions (kcal/mol)[b]			
			$\langle V^{el}_{l-s}\rangle_p$	$\langle V^{vdW}_{l-s}\rangle_p$	$\langle V^{el}_{l-s}\rangle_w$	$\langle V^{vdW}_{l-s}\rangle_w$
4[c]	−7.4	−6.8 ± 0.4	−73.2 ± 0.3	−79.6 ± 0.0	−71.9 ± 0.8	−44.3 ± 0.0
5[c]	−7.4	−8.6 ± 0.4	−75.6 ± 0.1	−93.9 ± 0.2	−71.8 ± 0.8	−53.2 ± 0.1
6[c]	−9.6	−9.1 ± 0.4	−67.2 ± 0.1	−85.9 ± 0.1	−64.5 ± 0.9	−40.6 ± 0.1
7 charged	nd	>−2.2[d]	−136.2 ± 1.1	−80.2 ± 0.4	−151.6 ± 0.6	−41.1 ± 0.3
7 neutral	nd	>0[e]	−64.6 ± 0.6	−84.5 ± 0.6	−70.6 ± 1.4	−43.2 ± 0.1
8	−9.7	−9.6 ± 0.3	−69.6 ± 0.1	−100.3 ± 0.9	−68.7 ± 0.2	−48.8 ± 0.3
10	−10.3	−8.5 ± 0.5	−72.0 ± 1.0	−111.6 ± 0.5	−76.4 ± 0.2	−56.4 ± 0.3
13	−11.3	−12.2 ± 0.4	−88.0 ± 0.3	−114.6 ± 0.4	−79.4 ± 0.3	−62.8 ± 0.8
15	−10.8	−10.1 ± 1.13	−73.3 ± 0.7	−132.5 ± 0.4	−81.4 ± 1.5	−62.0 ± 1.9
17	−9.3	−10.8 ± 0.5	−69.8 ± 0.5	−115.0 ± 1.1	−72.3 ± 0.2	−50.7 ± 0.0

[a] The experimental binding free energy calculated from experimentally determined K_i's using $\Delta G^0_{bind,exp} = RT \ln K_i$. [b] The calculated average electrostatic $\langle V_{el}\rangle$ and nonpolar $\langle V_{vdW}\rangle$ energies for ligand-surrounding (l−s) interactions. The subscripts *p* and *w* denote simulations of the ligand in complex with the protein and free in water, respectively. [c] Data from ref 19. [d] The calculated binding free energy of compound **7** in its charged form, corrected with the contribution of charged amino acids that were not taken into account in the simulation. [e] The calculated binding free energy of compound **7** in its neutral form, corrected for the cost of deprotonation at pH 4.5.

were determined in Plm I, Plm II, and Cat D enzyme inhibition assays. The measurements were performed at concentrations up to 1500 nM in the Plm I assay, 2500 nM in the Plm II assay, and 2000 nM in the Cat D assay. The results are given as K_i values in Table 1. All compounds in the series were devoid of activity in the Cat D assay, and all inhibitors with extended arms were also more active in the Plm I than in the Plm II assay. The hydroxyethylamine derivative **23**, previously prepared by our group,[18] was used as a reference compound in the Cat D assay and exhibited a $K_i = 30$ nM. Several of the compounds were >10-fold more active in the Plm I than in the Plm II assay. A comparison of the benzyl derivative **8** and the allyl derivative **6** shows that displacement of a benzyl group for an allyl group leads to a considerably lower activity in the Plm I assay, while the impact on the activity in the Plm II assay was much smaller. The allyl derivative **6** was the only inhibitor that was more active on Plm II than Plm I. With larger or more extended P1/P1′ substituents a significantly improved inhibition of Plm I could be accomplished, but the response in the Plm II assay was in general less pronounced. It is notable though, that smaller variations in the 4-position of the aromatic rings of the P1/P1′ side chain have a powerful effect on the ability to inhibit Plm II. Thus, **10** (unsubstituted), **11** (fluoro), **12** (methyl), and **13** (acetyl) exhibit Plm II K_i values of 29, 59, 129, and 6 nM, respectively. Reduction of one of the two amide bonds of **6** provided the amine **7** that was inactive in all enzyme assays.

Inhibition of Parasite Growth in Cell Culture. The ability to inhibit the growth of *P. falciparum* (clone 3D7) in human erythrocytes in vitro was determined for six compounds, **6**, **7**, **13**, **14**, **15**, and **19**, using a modification of a previously published procedure.[27] The results are presented as percent inhibition at 5 μM in Table 1. Compound **13**, the most active dual Plm I/Plm II inhibitor, was also the most active inhibitor of *P. falciparum* in culture demonstrating a 78% inhibition at 5 μM. Surprisingly, the amine **7**, which was inactive in the plasmepsin assays, exhibited a 50% inhibition at 5 μM, while the corresponding amide **6** was inactive in the cell culture assay.

Molecular Dynamics Simulations and Free Energy Calculations. The binding free energies of **7**, **8**, **10**, **13**, **15**, and **17** to Plm II were estimated using the linear interaction energy (LIE) method in combination with molecular dynamics simulations,[28] and the results for **4**, **5**, and **6** were taken from previous calculations.[19] A summary of the data is shown together with the experimental binding data in Tables 1 and 3. It is noteworthy that the calculated absolute binding free energies of all modeled compounds have a mean unsigned error of only 0.9 kcal/mol from the corresponding experimental value without any reparametrization of the LIE model.[29] Overall, the contribution to binding is clearly dominated by nonpolar interactions (all compounds display at least a 7 kcal/mol contribution to the binding free energy), the lipophilic compound **15** having the most favorable contribution, followed by **17** and **10**. However, as seen in Table 3, the electrostatic contributions to the binding free energies are smaller and not necessarily favorable. The polar compound **13** is the one with the best affinity in both the calculations and the assays, and it is the only compound with a more favorable electrostatic contribution to the binding free energy than **6**.

Interestingly, the terminal 4-acetyl groups of **13** are not directly involved in the increase in affinity. Instead, a change in binding conformation of this complex compared to that with **6** seems to account for the enhanced electrostatic interactions between the protein and the ligand. A striking difference between the binding modes of **6** and **13**, shown in Figure 3, is that in the former the allyloxy P1 chain extends into the S1 site of the enzyme, while in the latter the elongated chain with the 4-acetylphenyl group cannot be accommodated here. Rather, the chain makes a turn along the S1−S3 cleft, placing the phenyl where the P2 indan skeleton of **6** is situated, with its acetyl group extending into solution. Thus, the P2 indan system of **13** is relocated into the S2 pocket. This change in binding conformation was obtained for all simulated complexes with extended ligand P1/P1′ groups (**8**, **10**, **13**, **15**, and **17**).

The recent X-ray structure of Plm II in complex with the methylenedioxyphenyl-containing ligand EH58[22] shown in panel C of Figure 3 essentially agrees with our prediction of the placement of the P1′ group. The P1′ chain of **13** occupies the S1′ subsite and interacts with the hydrophobic side chains of Val78, Tyr192, Ile212, Thr221, Leu292, Phe294, and Ile300, while the P1 group in the S1−S3 cavity has nonpolar interactions with the side chains of Met15, Ile32, Tyr77, Phe111,

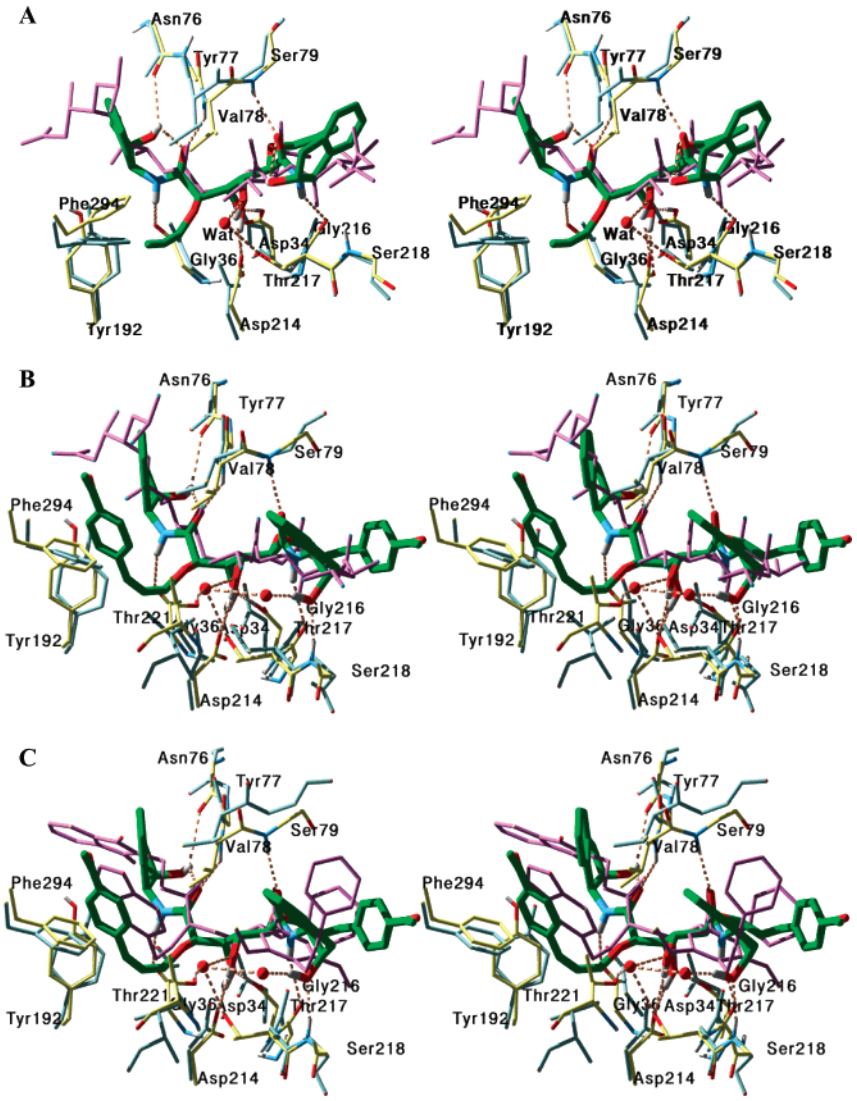

Figure 3. In panels A[19] and B an average MD structure is shown in stereo of the simulated compounds **6** (panel A, green, thick bonds) and **13** (panel B, green, thick bonds) in complex with Plm II (yellow) superimposed on the X-ray structure of Plm II (blue) in complex with pepstatin A (purple, 1SME[4]). Panel C shows an average MD structure in stereo of the simulated complex of **13** (green, thick bonds) and Plm II (yellow) superimposed on the X-ray structure of Plm II (blue) in complex with the hydroxyethylamine based inhibitor EH58 (purple, 1LF3[22]). For clarity reasons, all solvent molecules except one in panel A and two in panel B and C as well as many residues that have nonpolar interactions with the ligands were omitted in the figure. For the simulated complex, significant hydrogen bonds are indicated. The terminal P1/P1′ acetyl groups of **13** are highly rotatable and therefore appear distorted in the MD average structure.

Thr114, Phe120, Ile123, and the P2 indan system. A slight rotation of the Phe294 side chain and a displacement of the Gly291−Pro295 loop backbone accompany the accommodation of the P1′ chain of **13**, while the Met75−Val82 loop remains more or less in the crystallographic (1SME) starting position. The Gly291−Pro295 backbone displacement is also seen with the methylenedioxyphenyl **15**, while with the compounds with shorter P1′ side chains (**6**, **8**, **10**, and **17)** the Gly291−Pro295 backbone remains in the same conformation as in the X-ray structure with pepstatin A.[4] In the complex with **13**, the ligand backbone and the P2′ indan remain essentially in the same place during the simulation, following the direction of the pepstatin A backbone. The P2′ indan system is surrounded by the side chains of Ser37, Met75, Asn76, Leu131, Tyr192, and the backbone of Tyr77. Also, the P1′ side chain interacts with the indan system. On the other hand, the P2 indan moiety occupies the space located between the P2 and P4 groups of pepstatin A in the X-ray structure 1SME (Figure 3B). It is surrounded by the side chains of Val78, Ser79, Ala219, Ile 290, and the P1 side chain. Comparing the simulated conformation of **13** to the binding conformation of EH58 (Figure 3C),[22] the P2 indan system of **13** is predicted to be placed at the position between the benzyloxy and 3,5-dimethoxyphenyl groups of EH58.

The H-bonding interactions of the 1,2-dihydroxyethylene core structure, the backbone carbonyls, and the P2′ indan hydroxyl group of **13** are essentially identical to those found in the simulated complex of Plm II with **6**.[19] The active site water molecule found in the simulated complex with **6** (the leftmost water molecule in Figure 3B) is also present, bridging the interaction between the P1′ hydroxyl oxygen and the Thr217 side chain. Also, the intramolecular hydrogen bond found between the P2′ indan hydroxyl group and the P1′ carbonyl is present in the simulated complex with **13**.

However, the P2 indan system of **13** is rotated from its position in the complex with **6**, breaking the intramolecular H-bond between the indan hydroxyl and the P1 carbonyl. Instead, the P2 hydroxyl group accepts an H-bond from the amide nitrogen of Ser218 and donates one to a water molecule that bridges the interaction between the ligand and the Thr221 hydroxyl. Thus, the conformational change, resulting in strengthened ligand-surrounding electrostatic interactions, may be a plausible explanation of the higher affinities of the ligands with elongated P1/P1′ chains.

Compound **7** was found to be inactive, in agreement with the experimental results. Both the charged and uncharged forms of **7** were investigated. The charged form showed an ∼8 kcal/mol repulsive electrostatic contribution to its total binding free energy of about −2.2 kcal/mol, which corresponds to a K_i of about 25 mM. For the neutral form of **7**, after correction with the energy penalty that must be paid upon deprotonation of a charged compound with a pK_a ∼10 in a pH 4.5 solution, the total binding free energy is approximately +2 kcal/mol.

Discussion

Inhibitors comprising the C_2-symmetric 1,2-dihydroxyethylene scaffold with valine methylamide in the P2/P2′ positions (compounds **4** and **5**) were previously found by us to exhibit K_i values in the micromolar range against Plm II.[19] By a substitution with (1*S*,2*R*)-1-amino-2-indanol in the P2/P2′ positions (compound **6**) an increased affinity for Plm II of about 40 times was encountered.[19]

Since it has been shown that extended P1′ side chains can be accommodated in the S1′ subsite of Plm II,[11,22] we used the allyloxy substituent as a four-atom linker for extension in the trans position. A series of aromatic systems (**10**−**17**) were employed, resulting in very potent Plm I and Plm II inhibitors. It is also remarkable that six atom linkers between the scaffold and a phenyl (**18**, **20**), a carboxymethyl group (**19**), and a trimethylsilyl group (**21**) are all well tolerated. Apparently, both the P1 and P1′ side chains can be extended simultaneously. As suggested by the molecular dynamics simulations, on the prime side, the flexible S1′ subsite allows an elongated inhibitor to extend out into the solvent, abolishing any length restrictions of this chain. The simulations also predict that elongated P1 side chains can be aligned along the unobstructed S1−S3 cleft, displacing the P2 indan ring system from its position in S3 (as with compound **6**, Figure 3A) to the S2 pocket. This displacement results in a loss of an intramolecular H-bond and a gain of new H-bonding interactions with the protein and the solvent. A recently solved structure, ILF3, of Plm II in complex with an inhibitor containing a bulky methylenedioxyphenyl P1′ group confirms the quality of the models at these positions.[22] The LIE calculations reproduced the experimental values exceptionally well, without the need to reparametrize the LIE model.[29] Thus, the results indicate that the predicted binding conformation is a plausible model for further improvement of the inhibitors.

All of the compounds except **6** displayed higher affinities for Plm I than Plm II. Although no X-ray structure of Plm I has yet been solved, homology modeling suggests a somewhat more open binding cleft and a larger and more hydrophobic S3 subsite in Plm I compared to Plm II.[4,30] This is a possible explanation of why Plm II is less able to accommodate extended side chains, especially conformationally restricted ones such as in **17**.

Since the plasmepsins are active in an acidic food vacuole, we hypothesized that an amine function instead of an amide would be favorable for concentrating the molecules in the vacuole by protonation trapping. Reduction of one of the amides to the allyloxy amine **7** resulted in a total loss of activity in all three enzyme assays. According to the molecular dynamics simulations, this effect was shown to reside neither in loss of favorable ligand−protein interactions, nor in the increase in rotational degrees of freedom. Rather, the results suggest that it is the poorer solvation of the charged amine in the active site than in solution that is mainly responsible for the affinity loss. Although the assay was performed at pH 4.5, one cannot assume that the amine is protonated when bound to the enzyme. However, the effective affinity of the neutral form of **7**, after correction for pH, was found to be even lower than for the protonated form. According to the modeled complexes of Plm II and **7** the distance between the amine nitrogen and the catalytic aspartate carboxylate oxygens in the binding site of Plm II is at least 5 Å. Apparently, this is too far for efficient stabilization of the charge, especially since its hydrophobic immediate surrounding does not provide any favorable interactions for the charge. These results indicate that for an amine-containing ligand to be optimally active as an inhibitor, stabilization by, for example, carboxylate groups in the active site would be desirable. The tolerance of inhibitors incorporating the hydroxyethylamine mimic (e.g., compound **23**[18]) may possibly be explained by such interactions. Alternatively, the amine could be placed in a position so that it is in contact with bulk solvent, which would avoid any unfavorable desolvation effects. It is remarkable that, despite no activity in the enzyme assays, the amine **7** demonstrated a 50% inhibition of parasite growth at 5 μM on infected red blood cells. The inhibitory activity is possibly accounted for by inhibition of other proteases than Plm I/Plm II playing essential roles for the parasite replication.[31,32] Other explanations could be a totally different mechanism of action or, as suggested for chloroquine,[33] accumulation in the acidic food vacuole enhancing the activity in cell culture despite poor enzyme inhibition.[32]

Notably, in addition to the pico- to nanomolar inhibition constants, all compounds demonstrated selectivity versus the human aspartic protease Cat D. None of them showed any inhibitory effect on Cat D at concentrations up to 2000 nM, implying an at least 11- to 4000-fold selectivity. The structural basis of this selectivity will be the subject of future computational modeling and simulation studies.

Conclusion

We have employed fast microwave promoted palladium chemistry for making a series of C_2-symmetric inhibitors differing in the P1/P1′ positions. High affinity inhibitors of both Plm I and Plm II and with great selectivity toward the human Cat D were identified and

their binding conformations to Plm II were predicted by computer simulations. Regarding the malaria proteases Plm I and Plm II, a large variety of extended P1/P1′ side chains could be accommodated in the lipophilic S1−S3 groove and the flexible S1′ subsite. Despite the unsymmetrical binding sites these C_2-symmetric inhibitors were able to make sufficient binding interactions to afford K_i values in the pico- to nanomolar range. The best dual Plm I/Plm II inhibitor, compound **13**, exhibited K_i values of 0.8 and 6 nM, respectively. This compound was also the most active inhibitor of parasite growth in cell culture. A compound that is effective in inhibiting blood stage *P. falciparum*, but is devoid of activity in the Plm I and II assays, has been identified. No compounds were active as inhibitors of the human Cat D at concentrations up to 2000 nM, demonstrating a unique specificity for the plasmepsins versus the mammalian aspartic protease. To the best of our knowledge, these plasmepsin inhibitors represent the most selective reported to date.

Experimental Section

Chemistry. General Information. All microwave reactions were conducted in heavy-walled glass Smith process vials sealed with aluminum crimp caps fitted with a silicon septum. The microwave heating was performed in a Smith synthesizer single-mode microwave cavity producing continuous irradiation at 2450 MHz (Personal Chemistry AB, Uppsala, Sweden). Reaction mixtures were stirred with a magnetic stirring bar during the irradiation. The temperature, pressure, and irradiation power were monitored during the course of the reaction. After the completed irradiation, the reaction tube was cooled with high-pressure air until the temperature had fallen below 39 °C. ^{1}H and ^{13}C NMR spectra were recorded on a JEOL JNM-EX 270 spectrometer at 270.2 and 67.8 MHz, respectively, or on a JEOL JNM-EX400 spectrometer at 399.8 and 100.5 MHz, respectively. Chemical shifts are reported as δ values (ppm) indirectly referenced to TMS via the solvent residual signal. Optical rotations were obtained on a Perkin-Elmer 241 polarimeter. Specific rotations ($[\alpha]_D$) are reported in deg/dm, and the concentration (c) is given in g/100 mL in the specified solvent. Elemental analyses were performed by Mikro Kemi AB, Uppsala, Sweden. Flash column chromatography was performed on Merck silica gel 60, 0.04−0.063 mm. Thin-layer chromatography was performed using aluminum sheets precoated with silica gel 60 F_{254} (0.2 mm; E. Merck) and visualized with UV light, permanganate, or ninhydrin. Analytical RP-LC-MS was performed on a Gilson HPLC system with a Zorbax SB−C8, 5 μm 4.6 × 50 mm (Agilent technologies) column, with a Finnigan AQA quadropole mass spectrometer, at a flow rate of 1.5 mL/min. Preparative RP-LC-MS was performed on Gilson HPLC system with a Zorbax SB-C8, 5 μm 21.2 × 150 mm (Agilent technologies) column, with a Finnigan AQA quadropole mass spectrometer, at a flow rate of 15 mL/min.

(2*E*)-3-Bromo-2-propene-1-yl 2,2,2-trichloroethanimidate (24). Essentially, the procedure of Patil[34] was used. (*E*)-3-Bromo-2-propanol[35] (4.3 g, 31.4 mmol) was dissolved in CH_2Cl_2 (40 mL), and the solution was cooled to −10 °C. 50% Aqueous potassium hydroxide (40 mL) and tetra-*n*-butylammonium hydrogen sulfate (catalytic amount, 53 mg) was added. After 15 min of stirring, trichloroacteonitrile (1.2 equiv) was added dropwise. The resulting mixture was further stirred at −10 °C for 1.5 h and then allowed to attain room temperature in the next 1 h. The organic layer was separated, and the aqueous layer further extracted with CH_2Cl_2 (3 × 50 mL). The combined extracts were dried (Na_2SO_4) and concentrated to a reduced volume, and then filtered through a pad of Celite (4 cm). Concentration of the filtrate under reduced pressure gave **24** (8.7 g, 98%) as a clear liquid: ^{1}H NMR ($CDCl_3$) δ 8.39 (s, 1H), 6.57 (dt, J = 1.28, 13.69 Hz, 1H), 6.43 (dt, J = 5.90, 13.69 Hz, 1H), 4.76 (dd, J, 1.28, 5.90 Hz, 2H); ^{13}C NMR ($CDCl_3$) δ 162.2, 130.8, 111.2, 91.1, 68.2. Anal. ($C_5H_5BrCl_3NO$) C, H, N.

2,5-*O*-Bis((2*E*)-3-bromo-2-propen-1-yl)-L-mannaro-1,4:3,6-di-γ-lactone (25). l-1,4:3,6-Mannarodilactone (4.9 g, 5.8 mmol) was dissolved in dry dioxane (160 mL) under a nitrogen atmosphere. The mixture was heated until the dilactone was completely dissolved, and the solution was then allowed to attain room temperature. To the stirred solution were added trichloroacetimidate **24** (4.9 g, 17.2 mmol) and a catalytic amount of $BF_3 \times OEt_2$ (600 μL). The solution was stirred at room temperature for 1.5 h. After filtration through a pad of silica (3 cm), the filtrate was concentrated under reduced pressure. The crude product was washed with diethyl ether (3 × 80 mL) to give **25** (2.1 g, 89%) as white crystals: $[\alpha]_D^{22}$ −120° (c = 0.91, DMSO); ^{1}H NMR (DMSO-d_6) δ 6.73 (dt, J = 1.36, 13.57 Hz, 2H), 6.37 (dt, J = 6.39, 13.57 Hz, 2H), 5.27 (AA′ part of AA′XX′, 2H), 4.85 (XX′ part of AA′XX′, 2H), 4.28−4.13 (m, 4H); ^{13}C NMR (DMSO-d_6) δ 171.6, 133.5, 110.7, 74.7, 74.4, 68.8. Anal. ($C_{12}H_{12}Br_2O_6 \cdot {}^2/_3H_2O$) C, H.

(2*R*,3*R*,4*R*,5*R*)-*N*1,*N*6-Bis[(1*S*,2*R*)-2-hydroxy-1-indanyl]-2,5-bis[(2*E*)-3-bromo-2-propenyloxy]-3,4-dihydroxyhexane-1,6-diamide (9). The bislactone **25** (107 mg, 0.26 mmol) was dissolved in dry CH_2Cl_2 (8 mL) under a nitrogen atmosphere and cooled to 0 °C. (1*S*,2*R*)-1-Amino-2-indanol (155 mg, 1.04 mmol) was added rapidly. The reaction mixture was stirred at 0 °C for 1 h and then refluxed for 15 h. The solvent was removed under reduced pressure and subsequent purification by flash chromatography ($CHCl_3/CH_3OH$, 100:3) gave **9** (109 mg, 59%) as a light yellow solidified foam: $[\alpha]_D^{29}$ −16.7° (c 1.04, $CHCl_3$) ^{1}H NMR ($CDCl_3$) δ 7.34−7.21 (m, 10H), 6.49 (dt, J = 1.46, 13.68 Hz, 2H), 6.31 (dt, J = 6.18, 13.68 Hz, 2H), 5.29 (dd, J = 5.03, 8.83 Hz, 2H), 4.59 (ddd, J = 2.24, 5.03, 5.40 Hz, 2H), 4.23−4.11 (m, 8 H), 3.08 (dd, J = 5.40, 16.61 Hz, 2H), 2.82 (dd, J = 2.24, 16.61 Hz, 2H); ^{13}C NMR ($CDCl_3$) δ 171.2, 140.8, 139.7, 132.7, 128.6, 127.3, 125.5, 124.2, 110.5, 81.1, 72.6, 71.4, 70.9, 57.9, 39.3. Anal. ($C_{30}H_{34}Br_2N_2O_8$) C, H, N.

General Procedure for Preparation of the Compounds 10−17. Method I. A mixture of diamide **9** (40 mg, 0.056 mmol), 6 equiv of organoboronic acid, 2 M aqueous Na_2CO_3 (56.3 μL, 0.11 mmol), tetrakis(triphenylphosphine)palladium (8.37−12.2 mg, 0.0073−0.011 mmol), and DME/H_2O/EtOH, 12:4:3 (5 mL) was added to a heavy-walled Smith vial. The tube was capped and the mixture was stirred at 90 °C for 30 min in the microwave cavity. Purification by RP-LC-MS gave **10−17**.

(2*R*,3*R*,4*R*,5*R*)-*N*1,*N*6-Bis[(1*S*,2*R*)-2-hydroxy-1-indanyl]-2,5-bis[(2*E*)-3-phenyl-2-propenyloxy]-3,4-dihydroxyhexane-1,6-diamide (10). Compound **10** was prepared essentially according to method I, using diamide **9** (30 mg, 0.042 mmol), phenylboronic acid (31 mg, 0.25 mmol), 2 M aqueous Na_2CO_3 (42.3 μL, 0.085 mmol), tetrakis(triphenylphosphine)palladium (7.6 mg, 0.0066 mmol), and DME/H_2O/EtOH 12:4:3 (3 mL). Purification by RP-LC-MS (40 min gradient of 40−85% CH_3-CN in 0.05% aqueous formic acid) gave **10** (19 mg, 63%) as a white solid: $[\alpha]_D^{22}$ +16.4° (c 0.40, $CHCl_3$); ^{1}H NMR ($CDCl_3$) δ 7.42−7.14 (m, 20 H), 6.64 (dt, J = 1.24, 15.88 Hz, 2H), 6.27 (dt, J = 6.32, 15.88 Hz, 2H), 5.33 (dd, J = 5.03, 8.79 Hz, 2H), 4.68 (ddd, J = 2.01, 5.03, 5.45 Hz, 2H), 4.42−4.29 (m, 4H), 4.27 (AA′ part of AA′XX′, 2H), 4.23 (XX′ part of AA′XX′, 2H), 3.12 (dd, J = 5.45, 16.66 Hz, 2H), 2.95 (dd, J = 2.01, 16.66 Hz, 2H); ^{13}C NMR ($CD_3OD/CDCl_3$ 1:1) δ 175.1, 142.93, 142.91, 138.9, 136.4, 131.0, 130.5, 130.3, 129.4, 129.0, 127.6, 127.1, 126.6, 82.7, 75.2, 74.3, 73.6, 59.9, 42.1. Anal. ($C_{42}H_{44}N_2O_8 \cdot {}^1/_2H_2O$) C, H, N.

(2*R*,3*R*,4*R*,5*R*)-*N*1,*N*6-Bis[(1*S*,2*R*)-2-hydroxy-1-indanyl]-2,5-bis[(2*E*)-3-(4-fluorophenyl)-2-propenyloxy]-3,4-dihydroxyhexane-1,6-diamide (11). Compound **11** was prepared according to method I, using 4-fluorobenzeneboronic acid, and 9.9 mg (0.0086 mmol) of tetrakis(triphenylphosphine)palladium. Purification by RP-LC-MS (30 min gradient of 20−80% CH_3CN in 0.05% aqueous formic acid) gave **11** (19 mg, 46%) as a white solid: $[\alpha]_D^{22}$ +38.2° (c 0.62, CH_3OH); ^{1}H NMR

(CD_3OD) δ 7.43−7.36 (m, 4H), 7.29−7.10 (m, 8H), 7.04−6.97 (m, 4H), 6.66 (dt, J = 1.56, 15.97 Hz, 2H), 6.29 (dt, J = 6.27, 15.97 Hz, 2H), 5.38 (d, J = 5.08 Hz, 2H), 4.56 (ddd, J = 1.51, 5.08, 5.22 Hz, 2H), 4.35−4.25 (m, 4H), 4.22 (AA′ part of AA′XX′, 2H), 4.15 (XX′ part of AA′XX′, 2H), 3.16 (dd, J = 5.22, 16.52 Hz, 2H), 2.93 (dd, J = 1.51, 16.52 Hz, 2H); ^{13}C NMR (CD_3OD) δ 172.8, 162.5 (d, J_{CF} = 246.0), 140.8, 140.4, 133.1, 132.0, 128.1 (d, J_{CF} = 7.7), 127.7, 126.6, 124.9, 124.8 (d, J_{CF} = 2.1), 124.1, 115.0 (d, J_{CF} = 22.3), 79.8, 72.7, 71.2, 70.8, 57.3, 39.5. Anal. ($C_{42}H_{42}F_2N_2O_8$) C, H, N.

(2*R*,3*R*,4*R*,5*R*)-*N*1,*N*6-Bis[(1*S*,2*R*)-2-hydroxy-1-indanyl]-2,5-bis[(2*E*)-3-(4-tolyl)-2-propenyloxy]-3,4-dihydroxyhexane-1,6-diamide (12). Compound **12** was prepared according to method I, using *p*-tolylboronic acid, and 10.3 mg (0.0089 mmol) of tetrakis(triphenylphosphine)palladium. Purification by RP-LC-MS (30 min gradient of 30−87% CH_3CN in 0.05% aqueous formic acid) gave **12** (17 mg, 42%) as a white solid: $[\alpha]_D^{22}$ +38.2° (*c* 0.54, CH_3OH); ^{1}H NMR (CD_3OD) δ 7.28−7.19 (m, 10H), 7.16−7.06 (m, 6H), 6.63 (dt, J = 1.37, 15.88 Hz, 2H), 6.28 (dt, J = 6.36, 15.88 Hz, 2H), 5.37 (d, J = 5.03 Hz, 2H), 4.56 (ddd, J = 1.19, 5.03, 5.22 Hz, 2H), 4.34−4.26 (m, 4H), 4.22 (AA′ part of AA′XX′, 2H), 4.15 (XX′ part of AA′XX′, 2H), 3.15 (dd, J = 5.22, 16.43 Hz, 2H), 2.93 (dd, J = 1.19, 16.43 Hz, 2H), 2.30 (s, 6H); ^{13}C NMR (CD_3OD) δ 172.9, 140.8, 140.4, 137.5, 133.9, 133.5, 128.9, 127.7, 126.6, 126.3, 124.9, 124.1, 123.7, 79.8, 72.7, 71.4, 70.9, 57.3, 39.4, 19.9. Anal. ($C_{44}H_{48}N_2O_8 \cdot {}^1/_3H_2O$) C, H, N.

(2*R*,3*R*,4*R*,5*R*)-*N*1,*N*6-Bis[(1*S*,2*R*)-2-hydroxy-1-indanyl]-2,5-bis[(2*E*)-3-(4-acetylphenyl)-2-propenyloxy]-3,4-dihydroxyhexane-1,6-diamide (13). Compound **13** was prepared according to method I, using 4-acetylphenylboronic acid, and 10.5 mg (0.0091 mmol) of tetrakis(triphenylphosphine)-palladium. Purification by RP-LC-MS (30 min gradient of 10−75% CH_3CN in 0.05% aqueous formic acid) gave **13** (15 mg, 34%) as a white solid: $[\alpha]_D^{23}$ +17.5° (*c* 0.47, $CHCl_3$); ^{1}H NMR ($CDCl_3$) δ 7.90 (m, 4H), 7.42 (m, 4H), 7.37 (d, J = 8.70 Hz, 2H), 7.32−7.14 (m, 8H), 6.68 (dt, J = 1.37, 15.93 Hz, 2H), 6.38 (dt, J = 5.95, 15.93 Hz, 2H), 5.34 (dd, J = 5.08, 8.70 Hz, 2H), 4.68 (ddd, J = 2.11, 5.08, 5.49 Hz, 2H), 4.46−35 (m, 4H), 4.28 (AA′ part of AA′XX′, 2H), 4.25 (XX′ part of AA′XX′, 2H), 3.12 (dd, J = 5.49, 16.71 HZ, 2H), 2.94 (dd, J = 2.11, 16.71 Hz, 2H), 2.59 (s, 6H); ^{13}C NMR ($CDCl_3$) δ 197.6, 171.7, 140.9, 140.7, 139.7, 136.5, 132.7, 128.9, 128.6, 127.21, 127.18, 126.8, 125.6, 123.9, 82.0, 72.6, 72.2, 71.5, 58.0, 39.5, 26.7. Anal. ($C_{46}H_{48}N_2O_{10} \cdot {}^1/_2H_2O$) C, H, N.

(2*R*,3*R*,4*R*,5*R*)-*N*1,*N*6-Bis[(1*S*,2*R*)-2-hydroxy-1-indanyl]-2,5-bis[(2*E*)-3-(2,4-dimethoxy-3,5-pyrimidin)-2-propenyloxy]-3,4-dihydroxyhexane-1,6-diamide (14). Compound **14** was prepared according to method I, using 2,4-dimethoxypyrimidin-5-boronic acid, and 12.2 mg (0.0106 mmol) of tetrakis-(triphenylphosphine)palladium. RP-LC-MS (30 min gradient of 5−75% CH_3CN in 0.05% aqueous formic acid) did not give a total separation from side products. However, the pure title compound precipitated from the selected fractions and filtration gave **14** as white crystals (16 mg, 33%): $[\alpha]_D^{22}$ +29.8° (*c* 0.55, DMSO-d_6); ^{1}H NMR (DMSO-d_6) δ 8.39 (s, 2H), 7.79 (d, J = 8.88 Hz, 2H), 7.27−7.09 (m, 8H), 6.52 (dt, J = 1.24, 16.20 Hz, 2H), 6.41 (dt, J = 5.77, 16.20 HZ, 2H), 5.26 (dd, J = 5.03, 8.88 Hz, 2H), 5.12 (d, J = 4.30 Hz, 2H), 4.86 (AA′ part of AA′XX′, 2H), 4.43 (dddd, J = 1.19, 4.30, 4.67, 5.03 Hz, 2H), 4.23−4.10 (m, 4H), 4.06 (XX′ part of AA′XX′, 2H), 3.92 (s, 6H), 3.89 (s, 6H), 3.06 (dd, J = 4.67, 16.38 Hz, 2H), 2.81 (dd, J = 1.19, 16.38 Hz, 2H); ^{13}C NMR (DMSO-d_6) δ 171.7, 168.0, 164.3, 157.3, 142.6, 141.2, 128.4, 127.8, 126.8, 125.4, 123.1, 112.1, 79.7, 79.6, 72.7, 70.9, 70.3, 57.2, 55.1, 54.5. Anal. ($C_{42}H_{48}N_6O_{12} \cdot 1H_2O$) C, H, N.

(2*R*,3*R*,4*R*,5*R*)-*N*1,*N*6-Bis[(1*S*,2*R*)-2-hydroxy-1-indanyl]-2,5-bis[(2*E*)-3-(3,4-methylenedioxyphenyl)-2-propenyloxy]-3,4-dihydroxyhexane-1,6-diamide (15). Compound **15** was prepared according to method I, using 3,4-methylenedioxyphenylboronic acid and tetrakis(triphenylphosphine)palladium (11.5 mg, 0.010 mmol). Purification by RP-LC-MS (30 min gradient of 20−95% CH_3CN in 0.05% aqueous formic acid) gave **15** (16 mg, 37%) as a white solid: $[\alpha]_D^{21}$ +18.8° (*c* 0.49, $CHCl_3$); ^{1}H NMR ($CDCl_3$) δ 7.36 (d, J = 8.83 Hz, 2H), 7.31−7.16 (m, 8H), 6.94−6.88 (m, 2H), 6.83−6.74 (m, 4H), 6.55 (dt, J = 1.28, 15.79 Hz, 2H), 6.09 (dt, J = 6.50, 15.79 Hz, 2H), 5.97 (s, 4H), 5.34 (dd, J = 5.03, 8.83 Hz, 2H), 4.72 (ddd, J = 2.11, 5.03, 5.49 Hz, 2H), 4.28−4.18 (m, 8H), 3.16 (dd, J = 5.49, 16.66 Hz, 2H), 2.98 (dd, J = 2.11, 16.66 Hz, 2H); ^{13}C NMR ($CDCl_3$) δ 171.9, 148.0, 147.6, 140.8, 139.7, 134.1, 128.4, 127.0, 125.4, 123.9, 122.2, 121.6, 108.3, 105.8, 101.1, 81.5, 72.55, 72.49, 71.6, 57.9, 39.3. Anal. ($C_{44}H_{44}N_2O_{12} \cdot 1{}^1/_2H_2O$) C, H, N.

(2*R*,3*R*,4*R*,5*R*)-*N*1,*N*6-Bis[(1*S*,2*R*)-2-hydroxy-1-indanyl]-2,5-bis[(2*E*)-3-(3-thienyl)-2-propenyloxy]-3,4-dihydroxyhexane-1,6-diamide (16). Compound **16** was prepared according to method I, using 3-thiopheneboronic acid and 9.7 mg (0.0084 mmol) of tetrakis(triphenylphosphine)palladium. Purification by RP-LC-MS (30 min gradient of 30−85% CH_3CN in 0.05% aqueous formic acid) gave **16** (17 mg, 42%) as a white solid: $[\alpha]_D^{21}$ + 6.6° (*c* 0.37, $CHCl_3$); ^{1}H NMR ($CDCl_3$) δ 7.38 (d, J = 8.83 Hz, 2H), 7.31−7.25 (m, 6H), 7.21−7.15 (m, 8H), 6.64 (dt, J = 1.37, 15.84 Hz, 2H), 6.11 (dt, J = 6.41, 15.84 Hz, 2H), 5.32 (dd, J = 5.13, 8.83 Hz, 2H), 4.66 (ddd, J = 2.01, 5.13, 5.40 Hz, 2H), 4.38−4.19 (m, 8H), 3.11 (dd, J = 5.40, 16.61 Hz, 2H), 2.93 (dd, J = 2.01, 16.61 Hz, 2H); ^{13}C NMR ($CDCl_3$) δ 172.0, 141.0, 139.8, 138.8, 128.6, 128.5, 127.1, 126.4, 125.5, 125.1, 124.00, 123.96, 123.3, 81.7, 72.58, 72.55, 71.6, 58.0, 39.4. Anal. ($C_{38}H_{40}N_2O_8S_2$) C, H, N.

(2*R*,3*R*,4*R*,5*R*)-*N*1,*N*6-Bis[(1*S*,2*R*)-2-hydroxy-1-indanyl]-2,5-bis[(2*E*)-3-(2,5-dimethyl-3,4-oxazol)-2-propenyloxy]-3,4-dihydroxyhexane-1,6-diamide (17). Compound **17** was prepared according to method I, using 3,5-dimethylisoxazole-4-boronic acid, and 11.2 mg (0.0097 mmol) of tetrakis(triphenylphosphine)palladium. Purification by RP-LC-MS (30 min gradient of 20−75% CH_3CN in 0.05% aqueous formic acid) gave **17** (25.5 mg, 61%) as a white solid: $[\alpha]_D^{22}$ −6.4° (*c* 0.98, $CHCl_3$); ^{1}H NMR ($CD_3OD/CDCl_3$ 6:1) δ 7.91 (d, J = 8.83 Hz, 2H), 7.29−7.17 (m, 6H), 7.15−7.06 (m, 2H), 6.41 (dt, J = 1.33, 16.25 Hz, 2H), 6.04 (dt, J = 6.18, 16.25 Hz, 2H), 5.36 (dd, J = 5.03, 8.83 Hz, 2H), 4.57 (ddd, J = 1.37, 5.03, 5.17 Hz, 2H), 4.36−4.25 (m, 4H), 4.23 (AA′ part of AA′XX′, 2H), 4.13 (XX′ part of AA′XX′, 2H), 3.15 (dd, J = 5.17, 16.52 Hz, 2H), 2.93 (dd, J = 1.37, 16.52 Hz, 2H), 2.34 (s, 6H), 2.23 (s, 6H); ^{13}C NMR ($CD_3OD/CDCl_3$ 6:1) δ 172.7, 166.4, 158.5, 140.8, 140.4, 127.9, 126.8, 126.6, 125.0, 124.0, 121.0, 112.2, 79.8, 72.6, 71.6, 70.9, 57.3, 39.6, 10.5, 10.3. Anal. ($C_{40}H_{46}N_4O_{10}$) C, H, N.

(2*R*,3*R*,4*R*,5*R*)-*N*1,*N*6-Bis[(1*S*,2*R*)-2-hydroxy-1-indanyl]-2,5-bis[(2*E*,4*E*)-5-phenyl-pentadienyloxy]-3,4-dihydroxyhexane-1,6-diamide (18). A mixture of diamide **9** (40 mg, 0.056 mmol), styrene (103 μL, 0.90 mmol), *N*,*N*-diisopropylethylamine (58.8 μL, 0.34 mmol), *trans*-di(μ-acetato)bis[*o*-(di-*o*-tolylphosphino)benzyl]dipalladium (5.9 mg, 0.0063 mmol), DMF (0.85 mL), and H_2O (0.15 mL) was added to a heavy-walled Smith vial. The tube was capped and the mixture was stirred at 170 °C for 25 min in the microwave cavity. The reaction mixture was concentrated under reduced pressure and subsequent purification by flash chromatography ($CHCl_3/CH_3OH$, 100:1−100:2) gave **18** (20 mg, 46%) as a white solid: $[\alpha]_D^{22}$ +16.6° (*c* 0.78, $CHCl_3$); ^{1}H NMR (CD_3OD) δ 7.42−7.12 (m, 18H), 6.80 (dd, J = 10.48, 15.65 Hz, 2H), 6.55 (d, J = 15.65 Hz, 2H), 6.49 (dd, J = 10.48, 15.29 Hz, 2H), 5.92 (dt, 6.32, 15.29 Hz, 2H), 5.38 (d, J = 5.03 Hz, 2H), 4.59 (ddd, 1.60, 4.90, 5.03 Hz, 2H), 4.28−4.11 (m, 8H), 3.16 (dd, J = 4.90, 16.57 Hz, 2H), 2.94 (dd, J = 1.60, 16.57 Hz, 2H); ^{13}C NMR ($CDCl_3$) δ 171.8, 140.8, 139.8, 136.8, 134.6, 133.9, 128.6, 128.4, 127.9, 127.8, 127.6, 127.0, 126.5, 125.4, 124.0, 81.5, 72.5, 72.1, 71.5, 57.9, 39.3. Anal. ($C_{46}H_{48}N_2O_8$) C, H, N.

(2*R*,3*R*,4*R*,5*R*)-*N*1,*N*6-Bis[(1*S*,2*R*)-hydroxy-1-indanyl]-2,5-bis[(2*E*,4*E*)-5-(methoxycarbonyl)-pent-2,4-dienyloxy]-3,4-dihydroxyhexane-1,6-diamide (19). A mixture of diamide **9** (40 mg, 0.056 mmol), methyl acrylate (82 μL, 0.91 mmol), *N*,*N*-diisopropylethylamine (58.8 μL, 0.34 mmol), *trans*-di(μ-acetato)bis[*o*-(di-*o*-tolylphosphino)benzyl]dipalladium (5.6 mg, 0.0060 mmol), DMF (0.85 mL), and H_2O (0.15 mL) was added to a heavy-walled Smith vial. The tube was capped and the mixture was stirred at 150 °C for 30 min in the microwave cavity. The reaction mixture was concentrated under reduced

pressure, and subsequent purification by flash chromatography ($CHCl_3$/CH_3OH, 100:2) gave **19** (34 mg, 84%) as a white solid: ^{1}H NMR ($CDCl_3$) δ 7.35−7.17 (m, 12 H), 6.42 (dd, J = 10.97, 15.34 Hz, 2H), 6.12 (dt, J = 5.48, 15.34 Hz, 2H), 5.90 (d, J = 15.42 Hz, 2H), 5.31 (dd, J = 5.03, 8.82 Hz, 2H), 4.63 (ddd, J = 2.23, 5.03, 5.48 Hz, 2H), 4.38−4.28 (m, 4H), 4.26−4.14 (m, 4H), 3.75 (s, 6H), 3.11 (dd, J = 5.48, 16.66 Hz, 2H), 2.89 (dd, J = 2.23, 16.66 Hz, 2H); Approximately 5% of the tentatively assigned (*Z*)-coupled stereoisomer(s) could be traced as an impurity in the ^{1}H NMR spectra.^{13}C NMR ($CDCl_3$) δ 171.4, 167.1, 143.2, 140.7, 139.6, 136.5, 130.4, 128.5, 127.1, 125.4, 123.9, 122.1, 81.6, 72.5, 71.4, 71.0, 57.8, 51.6, 39.3. Anal. ($C_{38}H_{44}N_2O_{12}$) C, H, N.

(2*R*,3*R*,4*R*,5*R*)-*N*1,*N*6-Bis[(1*S*,2*R*)-2-hydroxy-1-indanyl]-2,5-bis[(2*E*)-5-phenyl-pent-2-en-4-ynyl]-3,4-dihydroxy-hexane-1,6-diamide (20). A mixture of diamide **9** (36 mg, 0.051 mmol), phenylacetylene (13 μL, 0.12 mmol), diethylamine (0.1 mL, 0.97 mmol), tetrakis(triphenylphosphine)-palladium (2.9 mg, 0.0025 mmol), CuI (0.97 mg, 0.0051 mmol), and DMF (0.9 mL) was added to a heavy-walled Smith vial. The tube was capped and the mixture was stirred at 120 °C for 10 min in the microwave cavity. The reaction mixture was concentrated under reduced pressure and subsequent purification by flash chromatography ($CHCl_3$/MeOH, 100:2) gave **20** (35 mg, 91%) as a white solid: $[\alpha]_D^{18}$ +21.8° (*c* 1.02, $CHCl_3$); ^{1}H NMR ($CDCl_3$) δ 7.44−7.39 (m, 4H), 7.36 (d, J = 8.83 Hz, 2H), 7.33−7.19 (m, 14H), 6.26 (dt, J = 5.86, 15.93 Hz, 2H), 6.03 (dt, J = 1.88, 15.93 Hz, 2H), 5.32 (dd, J = 5.08, 8.83 Hz, 2H), 4.63 (ddd, J = 2.29, 5.08, 5.40 Hz, 2H), 4.37−4.26 (m, 4H), 4.25−4.17 (m, 4H), 3.09 (dd, J = 5.40, 16.66 Hz, 2H), 2.88 (dd, J = 2.29, 16.66 Hz, 2H); ^{13}C NMR ($CDCl_3$) δ171.6, 140.9, 139.8, 137.5, 131.7, 128.48, 128.46, 128.4, 127.3, 125.5, 124.2, 123.0, 113.5, 91.1, 87.0, 81.6, 72.6, 71.5, 71.3, 57.9, 39.3. Anal. ($C_{46}H_{44}N_2O_8$) C, H, N.

(2*R*,3*R*,4*R*,5*R*)-*N*1,*N*6-Bis[(1*S*,2*R*)-2-hydroxy-1-indanyl]-2,5-bis[(2*E*)-5-trimethylsilyl-pent-2-en-4-ynyl]-3,4-dihydroxyhexane-1,6-diamide (21). A mixture of diamide **9** (40 mg, 0.056 mmol), trimethylsilylacetylene (19 μL, 0.13 mmol), diethylamine (0.1 mL, 0.97 mmol), tetrakis(triphenylphosphine)palladium (9.5 mg, 0.0082 mmol), CuI (1.07 mg, 0.0056 mmol), and DMF (0.9 mL) was added to a heavy-walled Smith vial. The tube was capped and the mixture was stirred at 90 °C for 30 min in the microwave cavity. The reaction mixture was concentrated under reduced pressure, and subsequent purification by RP-LC-MS (30 min gradient of 50−90% CH_3-CN in 0.05% aqueous formic acid) gave **21** (19 mg, 46%) as a white solid: $[\alpha]_D^{21}$ +7.35° (*c* 0.88, $CHCl_3$); ^{1}H NMR ($CDCl_3$) δ 7.29−7.21 (m, 10H), 6.21 (dt, J = 5.72, 16.02 Hz, 2H), 5.83 (dt, J = 1.92, 16.02 Hz, 2H), 5.30 (dd, J = 5.08, 8.79 Hz, 2H), 4.63 (ddd, J = 2.24, 5.08, 5.45 Hz, 2H), 4.30−4.20 (m, 4H), 4.18 (AA′ part of AA′XX′, 2H), 4.13 (XX′ part of AA′XX′, 2H), 3.11 (dd, J = 5.45, 16.57 Hz, 2H), 2.87 (dd, J = 2.24, 16.57 Hz, 2H), 0.19 (s, 18 H); ^{13}C NMR ($CDCl_3$) δ 171.5, 140.9, 139.7, 138.5, 128.5, 127.3, 125.5, 124.1, 113.4, 102.5, 96.5, 81.8, 72.6, 71.4, 71.2, 58.0, 39.4, −0.07. Anal. ($C_{40}H_{52}N_2O_8Si_2$) C, H, N.

(2*R*,3*R*,4*R*,5*R*)-*N*1,*N*6-Di[(1*S*,2*R*)-2-hydroxy-1-indanyl]-2,5-bis[(2*E*)-pent-2-en-4-ynyl]-3,4-dihydroxyhexane-1,6-diamide (22). To a stirred solution of compound **21** (16 mg, 0.021 mmol) in methanol (1.5 mL) was added $KF\times2H_2O$ (44 mg, 0.46 mmol). Since the reaction was slow, additional amounts of $KF\times2H_2O$ (190 mg, 2.0 mmol and 280 mg, 3.0 mmol after 4 and 7 h, respectively) were added. The reaction mixture was stirred at room temperature for 24 h. Thereafter, the solvent was removed under reduced pressure and the crude product was partitioned between $CHCl_3$ (5 mL) and H_2O (5 mL). The aqueous layer was extracted with $CHCl_3$ (2 × 5 mL), and the combined organic layers was washed with H_2O (2 × 5 mL), dried (Na_2SO_4), and concentrated to give **22** (13 mg, 97%) as a white solid: $[\alpha]_D^{22}$ +32.4° (*c* 0.55, 15% $CHCl_3$ in CH_3OH); ^{1}H NMR ($CDCl_3$) δ 7.33−7.21 (m, 10H), 6.27 (dt, J = 5.72, 15.97 Hz, 2H), 5.80 (ddt, J = 0.60, 2.52, 15.97 Hz, 2H), 5.31 (dd, J = 5.03, 8.70 Hz, 2H), 4.65 (ddd, J = 2.24, 5.03, 5.45 Hz, 2H), 4.30−4.24 (m, 4H), 4.20 (AA′ part of AA′XX′, 2H), 4.14 (XX′ part of AA′XX′, 2H), 3.12 (dd, J = 5.45, 16.66 Hz, 2H), 2.94 (d, J = 2.52 Hz, 2H), 2.89 (dd, J = 2.24, 16.66 Hz, 2H); ^{13}C NMR ($CDCl_3$) δ 171.4, 140.8, 139.5, 139.4, 128.5, 127.2, 125.4, 124.0, 112.2, 81.8, 81.0, 78.9, 72.5, 71.3, 71.0, 58.0, 39.3. Anal. ($C_{34}H_{36}N_2O_8\cdot1^1/_2H_2O$) C, H, N.

(2*R*,3*R*,4*R*,5*S*)-2,5-Di(allyloxy)-3,4-dihydroxy-6-[(1*S*,2*R*)-2-hydroxy-1-indanylamino]-*N*1-[(1*S*,2*R*)-2-hydroxy-1-indanyl]-hexanamide (7). The diamide **6** (194 mg, 0.35 mmol) in dry THF (2.5 mL) was added dropwise at −78 °C to a mixture of $LiAlH_4$ (56 mg, 1.6 mmol) in dry THF (1.5 mL). The suspension was allowed to attain room temperature and was thereafter refluxed for 48 h. The suspension was diluted with THF (10 mL) and 10% aqueous NaOH (40 mL) was added. The aqueous layer was separated and extracted with THF (4 × 10 mL). The combined organic layers were concentrated under reduced pressure, and the crude product was purified by RP-LC-MS (30 min gradient of 30−70% CH_3CN in 0.05% aqueous formic acid) to give **7** (15 mg, 9%) as a white solid: $[\alpha]_D^{22}$ +29.5° (*c* 1.00, $(CH_3)_2CO$); ^{1}H NMR ($(CD_3)_2CO$) δ 7.64 (d, J = 8.70 Hz, 1H), 7.44−7.37 (m, 1H), 7.30−7.14 (m, 7H), 6.01−5.86 (m, 2H), 5.36−5.22 (m, 3H), 5.14 (ddd, J = 1.36, 3.18, 10.43 Hz, 1H), 5.09 (ddd, J = 1.40, 3.38, 10.39 Hz, 1H), 4.64−4.51 (m, 2H), 4.22−4.10 (m, 6H), 4.06−3.96 (m, 2H), 3.78−3.55 (m, 1H), 3.19 (d, J = 4.99 Hz, 2H), 3.12 (dd, J = 4.95, 16.45 Hz, 1H), 3.05 (dd, J = 5.24, 16.25 Hz, 1H), 2.92 (dd, J = 3.13, 16.25 Hz, 1H), 2.89 (dd, J = 1.44, 16.45 Hz, 1H); ^{13}C NMR ($(CD_3)_2CO$) δ 173.1, 142.5, 142.4, 142.3, 141.7, 136.4, 135.3, 128.7, 128.4, 127.3, 127.2, 125.9, 125.8, 125.5, 125.0, 117.6, 116.5, 81.5, 78.3, 73.2, 72.7, 72.2, 71.9, 71.8, 71.4, 66.6, 57.9, 48.1, 40.6, 40.2. Anal. ($C_{30}H_{38}N_2O_7\cdot1^1/_3H_2O$) C, H, N.

Enzyme Assays and K_i Determinations. pro-Plm II was a generous gift from Helena Danielson (Department of Biochemistry, Uppsala University, Uppsala Sweden), and the expression and purification of Plm I will be published elsewhere (manuscript in preparation). Human liver Cat D was purchased from Sigma-Aldrich, Sweden. The activities of Plm I, Plm II, and Cat D were measured essentially as described earlier,[11] using a total reaction volume of 100 μL. The concentration of pro-Plm II was 3 nM, the amount of Plm I was adjusted to give similar catalytic activity, and 50 ng/mL pro-Cat D was used. The pro-sequence of Plm II was cleaved off by preincubation in assay reaction buffer (100 mM sodium acetate buffer (pH 4.5), 10% glycerol and 0.01% Tween 20) at room temperature for 40 min, and Cat D was activated by incubation in the same reaction buffer at 37 °C for 20 min. The reaction was initiated by the addition of 3 μM substrate (DABCYL-Glu-Arg-Nle-Phe-Leu-Ser-Phe-Pro-EDANS, AnaSpec Inc, San Jose, CA) and hydrolysis was recorded as the increase in fluorescence intensity over a 10-min time period, during which the rate increased linearly with time.

Stock solutions of inhibitors in DMSO were serially diluted in DMSO and added directly before addition of substrate, giving a final DMSO concentration of 1%. IC_{50} values were obtained by assuming competitive inhibition and fitting a Langmuir isotherm ($v_i/v_o = 1/(1+[I]/IC_{50})$) to the dose response data (Grafit), where v_i and v_o are the initial velocities for the inhibited and uninhibited reaction respectively and [I] is the inhibitor concentration.[36] The K_i was subsequently calculated by using $K_i = IC_{50}/(1+[S]/K_m)$[37] and a K_m value determined according to Michaelis−Menten.

Parasite Assay. Culture and synchronization of blood stages of *P. falciparum* (clone 3D7) was as previously described.[38] Assays evaluating the effects of compounds on parasite growth were performed using a modification of the [^{3}H]hypoxanthine incorporation assay described by Chulay et al.[27] Briefly, a highly synchronous culture containing early trophozoite stage parasites at ∼1% haematocrit and 1% parasitaemia was supplemented with [^{3}H]hypoxanthine (Amersham Biotech) to 10 μCi mL^{-1}, and then 50 μL aliquots were dispensed into wells of flat-bottomed 96-well microtiter plates. Wells were supplemented with an equal volume of medium containing various concentrations of test compound (1−5 μM final) or DMSO only (maximum final concentration 1% v/v). Plates were transferred to gassed boxes and cultured at 37 °C

for 30 h to allow parasite development through to mature schizont stage. Cultures were then harvested onto glass fiber filters (Filtermat A, Wallac, Turku, Finland) using a cell harvester. Filters were wetted with scintillation cocktail and bound radioactivity quantified in a β-counter. Control cultures containing established growth-inhibitory compounds or without parasites were included in each experiment. The amount of radioactivity in each sample was expressed relative to that in the control wells containing DMSO only. Four independent experiments were performed for each concentration of each test compound.

MD Simulations and Free Energy Calculations. The LIE method, described in detail elsewhere,[28,39] can be used to predict absolute binding free energies (ΔG_{bind}) of enzyme inhibitor complexes. A general version of the LIE formula can be written as

$$\Delta G_{bind} = \alpha(\langle V_{l-s}^{vdW}\rangle_p - \langle V_{l-s}^{vdW}\rangle_w) + \beta(\langle V_{l-s}^{el}\rangle_p - \langle V_{l-s}^{el}\rangle_w) + \gamma$$

where the electrostatic and van der Waals components of the ligand-surrounding interaction energies are denoted by the superscripts el and vdW, respectively. The subscripts *p* and *w* describe the ligand in complex with the solvated protein and free in water, respectively. Thus, in each binding calculation an MD simulation of the complex is performed as well as one of the free ligand in water. The averages are calculated as time averages from molecular dynamics trajectories. The LIE coefficients used in the model are the same as in earlier work.[19,29,40−43]

MD simulations were done using the program Q[44] and the force field parameters of GROMOS87.[45] AM1 calculations were performed to obtain partial charges for the P1 and P1′ side chains of the inhibitors, while the scaffold and P2/P2′ groups were assigned standard force field charges. The X-ray structure 1SME[4] of Plm II in complex with pepstatin A was used as a starting point for all simulations of the protein−ligand complexes, since this was the most relevant structure at the time being. Five internal water molecules found within 18 Å of the pepstatin A hydroxyl group were kept. To get reliable results from binding free energy calculations, it is necessary to use a correctly docked starting conformation of the protein−ligand complex. Since our previous study with the same scaffold predicted experimental binding affinities correctly,[19] we here employed the same procedure to produce starting conformations. Thus, the backbone of our ligands was superimposed onto the backbone of pepstatin A in the X-ray structure and the side chains were placed into the subsites (P1 into S1, etc.), guided by the X-ray structure.

Asp34, which is involved in a hydrogen bond with Asp214, was protonated at the oxygen interacting with Asp214. The Asp303 side chain was also protonated because of its hydrogen bond with the backbone oxygen of Ser215. Asp214 was assigned a negative charge. A simulation sphere for the molecular dynamics was defined with 20 or 18 Å radius, depending on ligand size and the center of simulation was chosen at the central hydroxyl oxygen of the ligand which is closest to the P1′ group. The system within the simulation sphere interacted with the system across the boundary only by bonds and angles. The simulation spheres were solvated in an SPC water grid with radius 20 or 18 Å accordingly. The minimum solute−solvent distance for the solvation procedure was set to 2.4 Å. Long-range electrostatics of the protein−solvent and solvent−solvent interactions were treated with the LRF[46] method, and the water was subjected to radial and polarization restraints[47] to mimic bulk water at the sphere boundary. MD simulations of the free ligands in water were set up using the same simulation sphere parameters and a central atom of the ligand was restrained to the center of the sphere by 100 kcal/mol Å^2 to keep the ligand from drifting toward the sphere boundary. In the simulation of the complex with the charged form of **7**, the solvent contained one (Na^+) counterion to maintain the same overall charge as in the simulation of the free ligand in water.[48] To account for the electrostatic interactions from charged protein groups outside the simulation sphere, a correction was added to the binding free energy of the protonated **7** using Coulomb's law with a high dielectric constant as reported in Åqvist et al.[48] For the neutral form of **7**, the free energy cost for deprotonation at a given pH_{exp} was calculated as $\Delta G = RT \ln 10(pK_a - pH_{exp})$ with the pK_a of the conjugate acid.

Each solvated protein−ligand system was relaxed for 1 ps at 1 K and then gradually heated to 300 K, equilibrated, and subjected to at least 1.35 ns molecular dynamics using a 1 fs time step. Energies were recorded every 10 fs. Energy averaging was done on ≥300 ps trajectories. A ≥2 ns simulation of each ligand in aqueous solution was performed under the same conditions as the protein simulation, and energy averaging was done on at least 800 ps trajectories. Longer simulation times were required for the free ligands than for the complexes due to higher energy fluctuations in water compared to the more conformationally restricted active site.

Acknowledgment. We thank the Swedish Foundation for Strategic Research (SSF), the National Graduate School of Scientific Computing (NGSSC), and the Swedish Research Council (VR) for financial support. We also thank Personal Chemistry for providing a Smith Synthesizer.

Note Added after ASAP Posting

An earlier version of this paper posted to the ASAP website December 9, 2003 contained errors in Scheme 1. The Scheme has been corrected in this new version posted December 12, 2003.

References

(1) Bremen, J. The Ears of the Hippopotamus: Manifestations, Determinants, and Estimates of the Malaria Burden. *Am. J. Trop. Med. Hyg.* **2001**, *64S*, 1−11.
(2) Werbovetz, K. A. Target-Based Drug Discovery for Malaria, Leishmaniasis, and Trypanosomiasis. *Curr. Med. Chem.* **2000**, *7*, 835−860.
(3) Banerjee, R.; Liu, J.; Beatty, W.; Pelosof, L.; Klemba, M.; Goldberg, D. E. Four Plasmepsins are Active in the *Plasmodium falciparum* Food Vacuole, Including a Protease with an Active-Site Histidine. *Proc. Natl. Acad. Sci. U.S.A.* **2002**, *99*, 990−995.
(4) Silva, A. M.; Lee, A. Y.; Gulnik, S. V.; Majer, P.; Collins, J.; Bhat, T. N.; Collins, P. J.; Cachau, R. E.; Luker, K. E.; Gluzman, I. Y.; Francis, S. E.; Oksman, A.; Goldberg, D. E.; Erickson, J. W. Structure and Inhibition of Plasmepsin II, a Hemoglobin-Degrading Enzyme from *Plasmodium falciparum*. *Proc. Natl. Acad. Sci. U.S.A.* **1996**, *93*, 10034−10039.
(5) Francis, S. E.; Sullivan, D. J., Jr.; Goldberg, D. E. Hemoglobin Metabolism in the Malaria Parasite *Plasmodium falciparum*. *Annu. Rev. Microbiol.* **1997**, *51*, 97−123.
(6) Berry, C. Plasmepsins as Antimalarial Targets. *Curr. Opin. Drug Discovery Dev.* **2000**, *3*, 624−629.
(7) Moon, R. P.; Tyas, L.; Certa, U.; Rupp, K.; Bur, D.; Jacquet, C.; Matile, H.; Loetscher, H.; Grueninger-Leitch, F.; Kay, J.; Dunn, B. M.; Berry, C.; Ridley, R. G. Expression and Characterization of Plasmepsin I from *Plasmodium falciparum*. *Eur. J. Biochem.* **1997**, *244*, 552−560.
(8) Carroll, C. D.; Patel, H.; Johnson, T. O.; Guo, T.; Orlowski, M.; He, Z.-M.; Cavallaro, C. L.; Guo, J.; Oksman, A.; Gluzman, I. Y.; Connelly, J.; Chelsky, D.; Goldberg, D. E.; Dolle, R. E. Identification of Potent Inhibitors of *Plasmodium falciparum* Plasmepsin II from an Encoded Statine Combinatorial Library. *Bioorg. Med. Chem. Lett.* **1998**, *8*, 2315−2320.
(9) Carroll, C. D.; Johnson, T. O.; Tao, S.; Lauri, G.; Orlowski, M.; Gluzman, I. Y.; Goldberg, D. E.; Dolle, R. E. Evaluation of a Structure-Based Statine Cyclic Diamino Amide Encoded Combinatorial Library Against Plasmepsin II and Cathepsin D. *Bioorg. Med. Chem. Lett.* **1998**, *8*, 3203−3206.
(10) Dolle, R. E.; Guo, J.; O'Brien, L.; Jin, Y.; Piznik, M.; Bowman, K. J.; Li, W.; Egan, W. J.; Cavallaro, C. L.; Roughton, A. L.; Zhao, W.; Reader, J. C.; Orlowski, M.; Jacob-Samuel, B.; DiIanni Carroll, C. A Statistical-Based Approach to Assessing the Fidelity of Combinatorial Libraries Encoded with Electrophoric Molecular Tags. Development and Application of Tag Decode-Assisted Single Bead LC/MS Analysis. *J. Comb. Chem.* **2000**, *2*, 716−731.
(11) Haque, T. S.; Skillman, A. G.; Lee, C. E.; Habashita, H.; Gluzman, I. Y.; Ewing, T. J. A.; Goldberg, D. E.; Kuntz, I. D.; Ellman, J. A. Potent, Low-Molecular-Weight Non-Peptide Inhibitors of Malarial Aspartyl Protease Plasmepsin II. *J. Med. Chem.* **1999**, *42*, 1428−1440.

(12) Jiang, S.; Prigge, S. T.; Wei, L.; Gao, Y.-E.; Hudson, T. H.; Gerena, L.; Dame, J. B.; Kyle, D. E. New Class of Small Nonpeptidyl Compounds Blocks *Plasmodium falciparum* Development In Vitro by Inhibiting Plasmepsins. *Antimicrob. Agents Chemother.* **2001**, *45*, 2577−2584.
(13) Nezami, A.; Luque, I.; Kimura, T.; Kiso, Y.; Freire, E. Identification and Characterization of Allophenylnorstatine-Based Inhibitors of Plasmepsin II, an Antimalarial Target. *Biochemistry* **2002**, *41*, 2273−2280.
(14) Asojo, O. A.; Afonina, E.; Gulnik, S. V.; Yu, B.; Erickson, J. W.; Randad, R.; Medjahed, D.; Silva, A. M. Structures of Ser205 Mutant Plasmepsin II from *Plasmodium falciparum* at 1.8 Å in Complex with the Inhibitors rs367 and rs370. *Acta Crystallogr. D* **2002**, *D58*, 2001−2008.
(15) Nöteberg, D.; Hamelink, E.; Hultén, J.; Wahlgren, M.; Vrang, L.; Samuelsson, B.; Hallberg, A. Design and Synthesis of Plasmepsin I and Plasmepsin II Inhibitors with Activity in *Plasmodium falciparum*-Infected Cultured Human Erythrocytes. *J. Med. Chem.* **2003**, *46*, 734−746.
(16) Dahlgren, A.; Kvarnstrom, I.; Vrang, L.; Hamelink, E.; Hallberg, A.; Rosenquist, A.; Samuelsson, B. Solid-Phase Library Synthesis of Reversed-Statine Type Inhibitors of the Malarial Aspartyl Proteases Plasmepsin I and II. *Bioorg. Med. Chem.* **2003**, *11*, 827−841.
(17) Oscarsson, K.; Oscarson, S.; Vrang, L.; Hamelink, E.; Hallberg, A.; Samuelsson, B. New Potent C2−Symmetric Malaria Plasmepsin I and II Inhibitors. *Bioorg. Med. Chem.* **2003**, *11*, 1235−1246.
(18) Nöteberg, D.; Schaal, W.; Hamelink, E.; Vrang, L.; Larhed, M. High-Speed Optimization of Inhibitors of the Malarial Proteases Plasmepsin I and II. *J. Comb. Chem.* **2003**, *5*, 456−464.
(19) Ersmark, K.; Feierberg, I.; Bjelic, S.; Hultén, J.; Samuelsson, B.; Åqvist, J.; Hallberg, A. C_2-Symmetric Inhibitors of *Plasmodium falciparum* Plasmepsin II: Synthesis and Theoretical Predictions. *Bioorg. Med. Chem.* **2003**, *11*, 3723−3733.
(20) Brik, A.; Wong, C.-H. HIV-1 Protease: Mechanism and Drug Discovery. *Org. Biomol. Chem.* **2003**, *1*, 5−14.
(21) Alterman, M.; Andersson, H. O.; Garg, N.; Ahlsen, G.; Lövgren, S.; Classon, B.; Danielson, U. H.; Kvarnström, I.; Vrang, L.; Unge, T.; Samuelsson, B.; Hallberg, A. Design and Fast Synthesis of C-terminal Duplicated Potent C(2)- Symmetric P1/P1′-Modified HIV-1 Protease Inhibitors. *J. Med. Chem.* **1999**, *42*, 3835−3844.
(22) Asojo, O. A.; Gulnik, S. V.; Afonina, E.; Yu, B.; Ellman, J. A.; Haque, T. S.; Silva, A. M. Novel Uncomplexed and Complexed Structures of Plasmepsin II, an Aspartic Protease from *Plasmodium falciparum*. *J. Mol. Biol.* **2003**, *327*, 173−181.
(23) Alterman, M.; Björsne, M.; Mühlman, A.; Classon, B.; Kvarnström, I.; Danielson, H.; Markgren, P.-O.; Nillroth, U.; Unge, T.; Hallberg, A.; Samuelsson, B. Design and Synthesis of New Potent C2−Symmetric HIV-1 Protease Inhibitors. Use of L-Mannaric Acid as a Peptidomimetic Scaffold. *J. Med. Chem.* **1998**, *41*, 3782−3792.
(24) Larhed, M.; Hallberg, A. Microwave-Assisted High-Speed Chemistry: A New Technique in Drug Discovery. *Drug Discovery Today* **2001**, *6*, 406−416.
(25) Larhed, M.; Moberg, C.; Hallberg, A. Microwave-Accelerated Homogeneous Catalysis in Organic Chemistry. *Acc. Chem. Res.* **2002**, *35*, 717−727.
(26) Herrmann, W. A.; Böhm, V. P. W.; Reisinger, C.-P. Application of Palladacycles in Heck Type Reactions. *J. Organomet. Chem.* **1999**, *576*, 23−41.
(27) Chulay, J. D.; Haynes, J. D.; Diggs, C. L. *Plasmodium falciparum*: Assessment of In Vitro Growth by [3H]Hypoxanthine Incorporation. *Exp. Parasitol.* **1983**, *55*, 138−146.
(28) Åqvist, J.; Luzhkov, V. B.; Brandsdal, B. O. Ligand Binding Affinities from MD Simulations. *Acc. Chem. Res.* **2002**, *35*, 358−365.
(29) Hansson, T.; Marelius, J.; Åqvist, J. Ligand Binding Affinity Prediction by Linear Interaction Energy Methods. *J. Comput.-Aided Mol. Des.* **1998**, *12*, 27−35.
(30) Radding, J. A. Development of Anti-Malarial Inhibitors of Hemoglobinases. *Annu. Rep. Med. Chem.* **1999**, *34*, 159−168.
(31) Coombs, G. H.; Goldberg, D. E.; Klemba, M.; Berry, C.; Kay, J.; Mottram, J. C. Aspartic Proteases of *Plasmodium falciparum* and other Parasitic Protozoa as Drug Targets. *Trends Parasitol.* **2001**, *17*, 532−537.
(32) Brinner, K. M.; Kim, J. M.; Habashita, H.; Gluzman, I. Y.; Goldberg, D. E.; Ellman, J. A. Novel and Potent Anti-Malarial Agents. *Bioorg. Med. Chem.* **2002**, *10*, 3649−3661.
(33) Sullivan, D. J., Jr.; Gluzman, I. Y.; Russell, D. G.; Goldberg, D. E. On the Molecular Mechanism of Chloroquine's Antimalarial Action. *Proc. Natl. Acad. Sci. U.S.A.* **1996**, *93*, 11865−11870.
(34) Patil, V. J. A Simple Access to Trichloroacetimidates. *Tetrahedron Lett.* **1996**, *37*, 1481−1484.
(35) Polt, R.; Sames, D.; Chruma, J. Glycosidase Inhibitors: Synthesis of Enantiomerically Pure Aza-Sugars from Schiff Base Amino Esters via Tandem Reduction-Alkenylation and Osmylation. *J. Org. Chem.* **1999**, *64*, 6147−6158.
(36) Copeland, R. A.; Editor *Enzymes: A Practical Introduction to Structure, Mechanism, and Data Analysis*; VCH: New York, 1996.
(37) Cheng, Y.; Prusoff, W. H. Relationship Between the Inhibition Constant (K1) and the Concentration of Inhibitor which Causes 50 Per Cent Inhibition (I50) of an Enzymatic Reaction. *Biochem. Pharmacol.* **1973**, *22*, 3099−3108.
(38) Blackman, M. J. Purification of *Plasmodium falciparum* Merozoites for Analysis of the Processing of Merozoite Surface Protein-1. *Methods Cell Biol.* **1994**, *45*, 213−220.
(39) Åqvist, J.; Medina, C.; Samuelsson, J. E. A New Method for Predicting Binding Affinity in Computer-Aided Drug Design. *Protein Eng.* **1994**, *7*, 385−391.
(40) Marelius, J.; Graffner-Nordberg, M.; Hansson, T.; Hallberg, A.; Åqvist, J. Computation of Affinity and Selectivity: Binding of 2, 4- Diaminopteridine and 2,4-Diaminoquinazoline Inhibitors to Dihydrofolate Reductases. *J. Comput.-Aided Mol. Des.* **1998**, *12*, 119−131.
(41) Graffner-Nordberg, M.; Kolmodin, K.; Åqvist, J.; Queener, S. F.; Hallberg, A. Design, Synthesis, Computational Prediction, and Biological Evaluation of Ester Soft Drugs as Inhibitors of Dihydrofolate Reductase from *Pneumocystis carinii*. *J. Med. Chem.* **2001**, *44*, 2391−2402.
(42) Brandsdal, B. O.; Åqvist, J.; Smalås, A. O. Computational Analysis of Binding of P1 Variants to Trypsin. *Protein Sci.* **2001**, *10*, 1584−1595.
(43) Luzhkov, V. B.; Åqvist, J. Mechanisms of Tetraethylammonium Ion Block in the KcsA Potassium Channel. *FEBS Lett.* **2001**, *495*, 191−196.
(44) Marelius, J.; Kolmodin, K.; Feierberg, I.; Åqvist, J. Q: A Molecular Dynamics Program for Free Energy Calculations and Empirical Valence Bond Simulations in Biomolecular Systems. *J. Mol. Graphics Modell.* **1998**, *16*, 213−225, 261.
(45) van Gunsteren, W. F.; Berendsen, H. J. C. *Groningen Molecular Simulation (GROMOS) Library Manual*; Biomos B. V.: Nijenborgh, Groningen, The Netherlands, 1987.
(46) Lee, F. S.; Warshel, A. A Local Reaction Field Method for Fast Evaluation of Long-Range Electrostatic Interactions in Molecular Simulations. *J. Chem. Phys.* **1992**, *97*, 3100−3107.
(47) King, G., Warshel, A. A Surface-Contained All-Atom Solvent Model for Effective Simulations of Polar Solutions. *J. Chem. Phys.* **1989**, *91*, 3647−3661.
(48) Åqvist, J. Calculation of Absolute Binding Free Energies for Charged Ligands and Effects of Long-Range Electrostatic Interactions. *J. Comput. Chem.* **1996**, *17*, 1587−1597.

JM030933G